Core Excitons and Vibronic Coupling in Diamond and Graphite

Y. Ma*
Physics Department, University of Washington, Seattle, Washington 98195

P. Skytt, N. Wassdahl, P. Glans, D. C. Mancini, J. Guo, and J. Nordgren
Physics Department, Uppsala University, Uppsala, Sweden
(Received 25 June 1993)

The C 1*s* exciton in diamond is studied by soft x-ray emission excited with high resolution monochromatic photons. A strong phonon sideband of 5 eV wide is observed in the exciton recombination spectrum. With the phonon contribution, the exciton binding energy is estimated to be 1.5 eV. The excited atom is suggested to undergo Jahn-Teller relaxation similar to that of the nitrogen impurities in diamond. A similar exciton is observed at the σ^*-band threshold in graphite. These results provide new insights to the understanding of the core exciton and the donor problem in diamond and other systems.

PACS numbers: 78.70.Dm, 71.35.+z, 71.55.Cn

The C 1*s* core exciton of diamond has attracted much attention recently [1–4]. This problem is interesting because it is a model system for the understanding of the core exciton and for testing electronic calculational methods; also it is related to the substitutional nitrogen impurity problem in diamond [5,6]. This is because in the equivalent core approximation (ECA) the excited core seen by the valence and conduction electrons is equivalent to that of a $Z+1$ atom, i.e., nitrogen. The core exciton in diamond was first observed by Morar *et al.*, in the C *K*-edge absorption spectrum [1]. They estimated that the exciton binding energy (BE) is about 0.2 eV and proposed to explain it using the effective mass approximation (EMA). Jackson and Pederson argued that the agreement with the EMA calculation is coincidental and suggested that there exists a deeper core exciton that is not observable in dipole transitions [2]. More recently Batson used the electron energy loss technique to probe the nondipole transitions. However, he did not observe the proposed deep exciton state [4], questioning the conclusion of the calculations [2].

In the related nitrogen impurity problem, the nitrogen donor level has been found to be about 1.7 eV [5]. This large value was suggested to be due to a large Jahn-Teller (JT) distortion around the impurity atom. Earlier electron paramagnetic resonance experiments and theories suggested that the nitrogen atom is shifted away from the center of its coordination tetrahedron by (10–40)% of the interatomic distances (1.54 Å), along a (111) direction [5]. However, there have been no direct structural determinations around the impurity atoms. In fact, a recent first principles calculation questioned the presence of the JT distortion [6]. Because of the growing interests in diamond films, especially in their semiconductor applications, it is important to clarify this controversy and to get a better understanding about the doping properties in diamond.

We investigated the core exciton in diamond using high resolution C *K* absorption and emission spectroscopy. From the C *K*-emission spectra obtained with high resolution photon excitation, a very strong vibronic coupling effect is shown to be present in the core exciton state. The vibronic coupling effect suggests a large shift (~0.20 Å) of the core excited atom from its equilibrium position in the ground state. The inclusion of the vibrational contribution puts the exciton BE at about 1.5 eV. These results suggest that the exciton is indeed similar to the nitrogen impurity problem and that they both undergo the suggested JT distortion. We also observed a sharp feature at the σ^*-band absorption threshold of graphite which we believe is a core exciton state [7]. Similar to the diamond results, it also exhibits strong vibronic coupling effects. These results suggest that the ECA can be generally applied to the core exciton problems and, together with the vibronic coupling effects, have broad implications in the x-ray spectra and impurity problem of other systems, such as C_{60}.

The measurements were performed at the beam line X1B of the National Synchrotron Light Source. The experimental details were similar to those described in another paper [8]. The C *K*-edge absorption spectrum was obtained by photoelectron yield and the emission spectra were obtained with a grating spectrometer. Two diamond samples, one of type IIa and one type IIb, were measured with nearly identical results. The graphite sample is a highly oriented pyrolytic graphite. The energy of the spectrometer was calibrated using the Zn *L*-emission energies, while the incident photon energy is obtained from the spectrometer using the specular reflection. The energy resolution of the spectrometer was set at about 0.9 eV, and that of the incident photon was about 0.3 eV.

The absorption and emission spectra for diamond are shown in Fig. 1. The emission from the valence bands had been discussed elsewhere [8] and the valence band maximum (VBM) is found at approximately 284.0 eV. The emission intensity beyond the VBM is then assigned to the recombination transition. It is clear from Fig. 1(a) that the exciton in the absorption spectrum is at about 289.5 which is more than 5 eV above the VBM, not the

0031-9007/93/71(22)/3725(4)$06.00

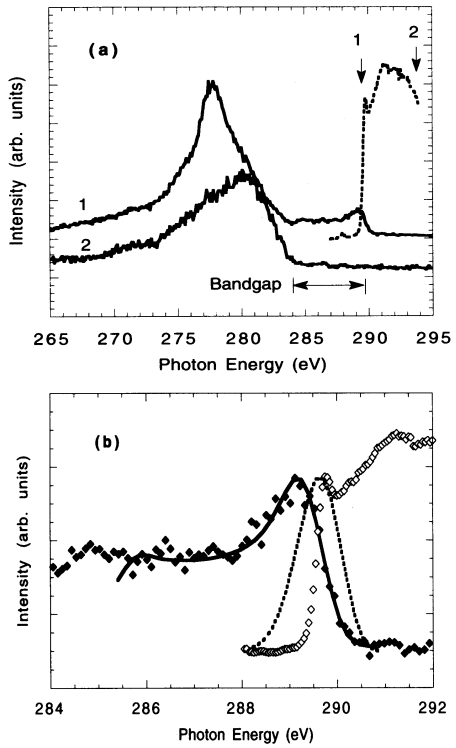

FIG. 1. (a) C K-edge absorption (dashed) and emission (solid curves) spectra of diamond. The emission spectra are measured with excitation energy of 289.6 (curve 1) and 294.5 eV (curve 2), respectively. (b) The absorption and emission spectra in the band-gap region: Experimental emission (filled diamonds) and absorption (open diamonds) spectra. The solid line represents the Franck-Condon phonon spectra calculated with $Q_0=0.2$ Å and $n=8$, and broadened by a Gaussian of FWHM $=0.9$ eV. The dashed curve represents the phonon broadened excitation peak with $Q_0=0.2$ Å.

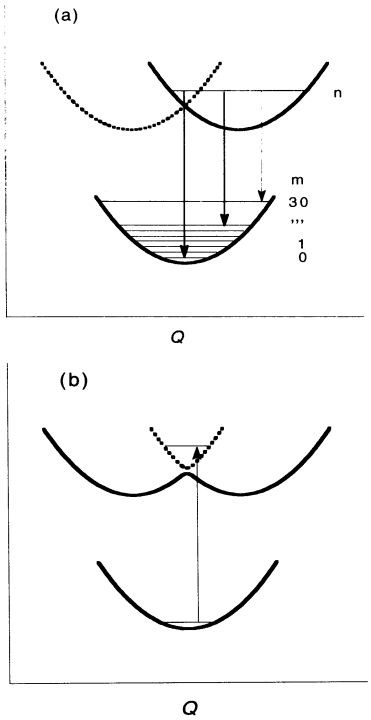

FIG. 2. Potential-energy surfaces plotted along C-C stretching directions: (a) in localized representation (broken symmetry) and (b) in delocalized or nonbroken symmetry representation. The upper curves are for the excitonic states and the lower curves for the ground state. The gap between the upper dashed and solid curves in (b) is due to vibronic coupling (see Ref. [12]). The arrows indicate the absorption (b) or emission (a) transitions.

4.3 eV obtained in Ref. [3]. Note also that the exciton in the emission spectra has not been observed without using the direct excitation [3,9]. The recombination spectrum is composed of a peak at about 289 eV and a long tail which fills the whole band-gap region. This special spectral shape can be attributed to the phonon excitations accompanying the recombination transition. Since the maximum phonon frequency in diamond is 0.16 eV (the C-C stretching vibrations), the width of this phonon sideband suggests that vibration numbers as high as 35 are excited in the recombination process.

Within the Born-Oppenheimer approximation, phonon excitation accompanying electronic transitions are well understood [10,11]. The basic principle is illustrated in Fig. 2(a), where the vibrational potential-energy curves of two electronic configurations are drawn. The intensities of the phonon excitation are determined by the Franck-Condon (FC) factors, $|\int \chi_m(Q)\chi'_n(Q-Q_0)dQ|^2$, where χ_m (χ'_n) is the mth (nth) vibrational wave function of the lower (upper) state. Q is the appropriate coordinate, such as the C-C stretching coordinate, and Q_0 is the shift in the equilibrium coordinate between the two electronic states. In the case of the emission transition, the upper or initial state is the excitonic state, while the lower or the final state is the ground state.

To simulate the phonon spectrum, we used harmonic potentials and a single vibrational mode (the C-C stretching mode with $\hbar\omega=0.16$ eV) for both states. For given n and Q_0, FC factors are calculated for $m=0$ to 30. The result is then broadened by a Gaussian with a full width at half maximum of 0.9 eV to simulate the energy resolution of the spectrometer and the lifetime broadening of the exciton state. Good agreements with experiments are obtained at around $Q_0=0.20$ Å and $n=8$. Because of the concern for the validity of the harmonic approximation, the calculation did not go beyond $m=30$. To get a better estimate for these parameters, we need to go beyond the harmonic approximation and to understand the vibronic coupling effects in the absorption and emission processes. Qualitatively, however, it is clear that the shift in equilibrium coordinate (Q_0) and the initial vibration number (n) needs to be large to explain the shape of the phonon sideband. For small Q_0 or n, the phonon spectrum is of Poisson or Gaussian shape.

The large phonon sideband then suggests that (1) compared with the ground state, the bond length between the core excited carbon atom and its neighbors changed by about 15%; (2) the exciton BE is much more than previously estimated: to the separation of 0.2 eV between the exciton peak and the conduction band minimum in the absorption spectrum [1], we need to add the vibrational contributions, $n\hbar\omega$, putting the BE at about $8\times0.16+0.2$ eV $=1.5$ eV. This revised picture of the exciton is much more like that of the substitutional nitrogen impurities, i.e., a donor level of 1.7 eV and the nitrogen atom occupying an off-center position. From this similarity, we suggest that the core excited carbon C* atom is probably shifted away from one of its nearest neighbors along the (111) direction. The photoelectron occupies an antibonding σ^* type of orbital, which accounts for the lengthening of the bond.

There is a problem in this seemingly perfect agreement between the properties of the core exciton and the nitrogen impurity: The large shift in the equilibrium coordinate Q_0 between the upper and lower states also implies that the exciton peak in the excitation spectrum should be broad, as indicated in Fig. 1(b). The broadening is again obtained from the FC factors, $|\int\chi_0(Q)\chi_n'(Q-Q_0)dQ|^2$. Here because the vibrational energy is much more than the thermal energy at room temperature, the initial state of the system is assumed to be in the vibrational ground state. The excitation peak should have a width of more than 1 eV, much more than the width of the measured exciton peak in the absorption spectrum ($\sim$0.2 eV) [1]. This disagreement suggests that the potential surfaces of the exciton state are different in the absorption and the emission processes.

This apparent contradiction may be explained by the vibronic coupling effects in the exciton states because, similar to the nitrogen impurity problem, we expect strong JT effects in the exciton state. Our discussion is illustrated by the potential-energy curves in Fig. 2, which have been used to discuss the vibronic coupling and symmetry breaking in core excited CO_2 and ethylene molecules [12]. For diamond, Fig. 2 shows only a cross section of the potential-energy surfaces along two C-C bond directions. The exciton may be described in two different pictures. In the localized picture, the photoelectron is assumed to be localized on one of the four C-C bonds, resulting in four degenerate states. The potential-energy surfaces of the excited states are displaced as shown in Fig. 2(a). The symmetry of the excitonic state is lower than that of the ground state. In the symmetry adapted or delocalized representation, where the electron is delocalized over the four C-C bonds, four entirely different potential-energy surfaces can be constructed. These potential surfaces are coupled via vibrations, such as the C-C stretching mode. The potential-energy curve corresponding to a configuration with a totally symmetric electronic wave function is shown by the solid curve in Fig. 2(b), while the dashed curve corresponds to a configuration with a non-totally-symmetric electronic wave function. The vibronic coupling effects also open an energy gap between the two states [12]. For our following model, it is important to emphasize the vibronic coupling nature of these potential-energy surfaces. A symmetric arrangement of the atoms will dictate a symmetric electronic wave function, and vice versa.

In the absorption process, the system is excited into the symmetry adapted states as shown in Fig. 2(b). This is because in the ground state the carbon atoms are arranged in a symmetric arrangement. Since the absorption process occurs on a very fast time scale (about 10^{-16} s) relative to the nuclear motion (about 10^{-14} s), the atoms maintain the same arrangement during the absorption process. The photoelectron is forced into a symmetry adapted state, i.e., it is delocalized over the four C-C bonds. Because the electronic wave function of the ground state (C 1s) is totally symmetric, transition to the totally symmetric electronic state is not dipole allowed [13]. The absorption process can only excite the system to the non-totally-symmetric states, e.g., the upper dashed state in Fig. 2(b). After the transition, because of the threefold degeneracy of these excited states, the system begins to undergo the JT distortion: The photoelectron becomes localized along one of the C-C bonds and, at the same time, the excited atom begins to move to an off-center position. The potential-energy surface then switches to one of the localized potential-energy surface [the solid upper curve in Fig. 2(a)]. From there the emission process takes place. Note that because of the short core hole lifetime, there will not be enough time for the excited atom to relax to the vibrational ground state of $n=0$ before the emission and there exists a long phonon sideband in the emission spectrum.

It is interesting to note that the nature of the C 1s exciton is similar to the valence excitons in alkali halide, especially the self-trapped excitons (STE) [14,15]. The STE is also found to relax to an off-center configuration upon creation. However, because of the relatively long exciton lifetime, 10^{-2}–10^{-9} s [14], the vibrational relaxation process in these systems can be followed. Depending upon the exciton lifetime, thus the degree of relaxation, different Stokes shifts are observed in the emission bands. In fact, this relaxation process has been studied by time resolved measurements [15].

In the above picture the core exciton, after taking into account the vibronic effects, is well described by the equivalent core approximation. This result has important implications in our understanding of donor levels and core excitons in other systems, such as Si and C_{60} materials. Indeed we have observed a sharp feature at the σ^*-band threshold of graphite, as indicated in Fig. 3. The details of the graphite results will be discussed elsewhere [16]. The peak observed at the σ^*-band absorption threshold at 291.65 eV shows the same polarization dependence as the σ^* band. In earlier absorption measurements this peak was not well resolved and was probably taken as a

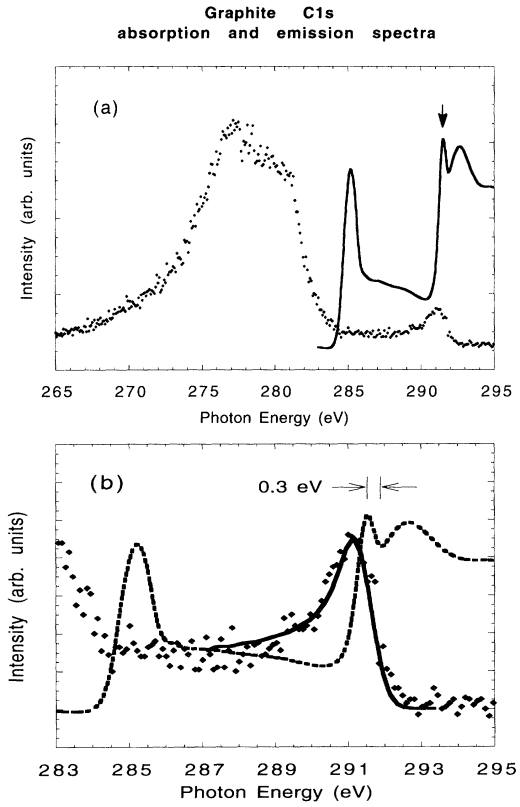

FIG. 3. (a) C K-edge absorption (solid) and emission (dots) spectra of graphite. The arrow indicates the peak assigned to the core exciton. (b) The spectra in the exciton region: emission (dots) and absorption (dashed). The solid line is the Franck-Condon phonon spectrum calculated with $n=10$, and $Q_0=0.25$ Å. The exciton peak in the absorption spectrum is estimated to be 0.3 eV below that σ^*-band threshold; see also Ref. [7].

feature of the conduction band [17,18]. Our high resolution measurement shows that the feature is very sharp, with width of about 0.5 eV [7]. Because of the sharpness, this peak is not likely a conduction band state, as suggested in Ref. [7]. The peak predicted in the band calculations is believed to be that of the broader peak at 292.5 eV [18]. In fact, the emission spectrum shows a recombination peak at this energy with long phonon tail, as shown in Fig. 3(b). This peak resonates with the peak in the absorption spectrum, indicating that the new feature is a very localized state, supporting the core exciton assignment. Following the diamond example, the phonon sideband in the emission spectrum suggests that there is also strong vibronic coupling effects in graphite as well. In this case the photoelectron presumably occupies an antibonding σ^* bond in the plane, along one of the three C-C bonds. This bond consequently lengthens and the trigonal symmetry of the ground state is broken. Using the highest phonon frequency of $\hbar\omega=0.2$ eV, the binding energy of this exciton is estimated to be $n\hbar\omega+0.3=10\times0.2+0.3$ eV $=2.3$ eV, and the distortion is estimated at 0.25 Å.

In conclusion, soft x-ray emission spectroscopy revealed a new picture of the core exciton and the existence of strong vibronic coupling effects in diamond, which is also observed in graphite. Including the vibronic coupling effect, the equivalent core approximation is found to be generally adequate in modeling the core excitons. Using the ECA, we also confirmed the substantial trigonal distortions around substitutional nitrogen impurities in diamond and give an estimate of the distortion. We proposed a model to interpret the different vibrational excitations observed in the emission and absorption spectra of diamond by the time scales of the absorption, emission, and vibrational relaxation processes.

We would like to thank F. Brown for useful discussions about the valence excitons. This work is supported in part by the Swedish Natural Science Research Council. The National Synchrotron Light Source is operated under DOE Contract No. DE-AC02-76CH00016.

*Also at Molecular Science Researcl. Center, Pacific Northwest Labs, Richland, WA 99352.

[1] J. F. Morar *et al.*, Phys. Rev. Lett. **54**, 1960 (1984).
[2] K. A. Jackson and M. R. Pederson, Phys. Rev. Lett. **67**, 2521 (1991).
[3] J. Nithianandam, Phys. Rev. Lett. **69**, 3108 (1992).
[4] P. E. Batson, Phys. Rev. Lett. **70**, 1822 (1993).
[5] See, e.g., J. Walker, Rep. Prog. Phys. **42**, 108 (1979); G. Davies, *ibid.* **44**, 788 (1981).
[6] K. Jackson, M. R. Pederson, and J. G. Harrison, Phys. Rev. B **41**, 12641 (1990).
[7] P. Batson, Phys. Rev. B **48**, 2608 (1993); and L. J. Terminello *et al.*, Chem. Phys. Lett. **182**, 491 (1991), also observed this feature.
[8] Y. Ma *et al.*, Phys. Rev. Lett. **69**, 2598 (1992).
[9] M. Umeno and G. Wiech, Phys. Status Solidi (b) **59**, 145 (1973).
[10] G. Mahan, Phys. Rev. B **15**, 4587 (1977); C. O. Almbaldh, *ibid.* **16**, 4343 (1977).
[11] A. Mansour and S. E. Schnatterly, Phys. Rev. Lett. **59**, 567 (1987). However, recent results by W. L. O'Brien *et al.* [*ibid.* **70**, 238 (1993)] questioned the interpretation of the phonon sidebands.
[12] W. Domcke and L.S. Cederbaum, Chem. Phys. **25**, 189 (1977); F. X. Gadea *et al.*, Phys. Rev. Lett. **66**, 883 (1991).
[13] This type of selection rule argument for the C 1s spectra in diamond was first used in Ref. [2].
[14] N. Itoh, Adv. Phys. **31**, 491 (1982); R. T. Williams, and K. S. Song, J. Phys. Chem. Solids **51**, 679 (1990).
[15] R. T. Williams *et al.*, Phys. Rev. Lett. **66**, 2140 (1991).
[16] P. Skytt, N. Wassdahl, P. Glans, J. Guo, J. Nordgren, and Y. Ma (unpublished).
[17] G. Comelli *et al.*, Phys. Rev. B **38**, 7511 (1988); D. A. Fisher *et al.*, Phys. Rev. B **44**, 1427 (1991).
[18] N. A. W. Holzwarth, S. G. Louie, and R. Rabii, Phys. Rev. B **26**, 5382 (1982); X. Weng, P. Rez, and H. Ma, Phys. Rev. B **40**, 4175 (1989).